



THE HEIM COLUMN

A Low Heat Leak Temperature Stabilized Support

J. R. Heim

December 10, 1971

ABSTRACT

The design and analysis of a low heat leak temperature stabilized column type support is presented. Engineering design formulas have been developed for a three tube composite column which uses the cryostat liquid nitrogen radiation shield as a heat sink. Also, the design concept and method of analysis for the general case using many tubes with or without heat sinks is also developed. These simple structural elements conduct negligible amounts of heat to the supported cold mass and may be designed to shrink, grow or remain unchanged in height when cooled to operating conditions. The three tube specimen presented herein has a collapse load of 9,000 Kg and a heat leak of less than eleven milliwatts.



## INTRODUCTION

Most superconducting magnet coils operate in a liquid helium environment at temperatures near 4°K. Since the operating efficiency of these devices is directly related to the heat transferred into the helium pool, much cryostat design effort is devoted to minimizing heat leaks. One of the major heat leak paths for a large superconducting magnet is the primary structure which supports the cold mass. The composite column described herein has been designed to be used as such with good load carrying capability and low heat leak. The test specimen shown in Fig. 1 has been

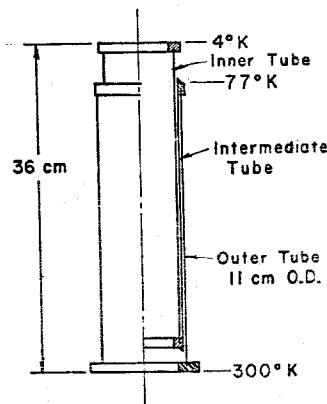


Fig. 1 Test Specimen

sized to carry a 1,000 Kg axial load at 4°K with a heat leak of less than 11 milliwatts and no shrinkage when cooled down. The top end of the column is attached to a liquid helium chamber and the bottom end is attached to the vacuum jacket wall at room temperature. The joint between the intermediate and outer tubes is thermally sunked to a liquid nitrogen radiation shield at 77°K.

### THREE TUBE COLUMN

This example is the basic form of a composite column in that a minimum number of tubes have been used and the intermediate tube is forced to a sink temperature.

#### Design Concept

The column shown is made with 3 tubes and the following considerations:

Geometry Consideration. A decrease of the intermediate tube length will increase the overall column height.

Materials Consideration. The individual tubes may be made from different materials with correspondingly different thermal expansion coefficients.

If one selects materials such that the thermal contraction of the intermediate tube is equal to the sum of the contractions of the inner and outer tubes, the overall column height will not change when the column is cooled down to operating conditions. Thus, all alignments may be done when the magnet is installed and the alignments will not be lost when the magnet is cooled down.

For superconducting magnet coil support applications an excellent combination of inexpensive materials may be chosen which satisfies the above temperature considerations and also has low heat conduction. The inner and outer tubes are made of epoxy glass laminates and the intermediate tube is made of aluminum. Both materials are readily available in a wide variety of tube sizes.

### Construction Details

The test specimen shown was constructed using 6061 T6 aluminum for the intermediate tube and NEMA grade G-10<sup>1</sup> epoxy fiberglass for the inner and outer tubes. Both G-10 tubes have a .16 cm wall thickness since this was the thinnest tube wall thickness manufactured using normal shop practice. A .32 cm wall thickness was chosen for the aluminum tube to assure good tube-to-flange welds. Four aluminum flanges were machined with .6 cm deep grooves to accept the G-10 tubes and two of these flanges were welded to both ends of the aluminum tube as shown in Fig. 2. Prior to bonding

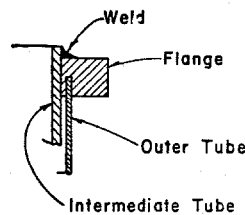


Fig. 2 Typical Joint

with epoxy all aluminum bonding surfaces were chemically etched with a sodium dichromate sulfuric acid solution while the G-10 bonding surfaces were lightly sanded and wiped with a cleaning agent. All aluminum to G-10 joints were bonded together with a low temperature epoxy<sup>2</sup>. Also, temporary spacers were used between tubes to maintain concentricity while the epoxy cured. After curing, the top and bottom flange surfaces were final machined perpendicular to the column center line.

Thermal Analysis

Computation of the heat transferred up the inner tube and into the helium chamber is fairly straight forward. Several layers of superinsulation were wrapped on all surfaces to limit radiant heat transfer. Therefore, radiant heat transfer was neglected to simplify analysis. The thermal conductivity of aluminum is much greater than that of epoxy glass laminates, therefore, the aluminum tube was assumed to be an isothermal surface. Since the thermal conductivity of epoxy glass laminates is fairly constant at low temperatures, Fouriers conduction equation may be integrated directly to yield the familiar form

$$\dot{Q} = -kA \frac{T_T - T_B}{\ell_3}$$

where  $\dot{Q}$  = heat flow into helium chamber

$k$  = thermal conductivity of inner tube

$A$  = cross sectional area of inner tube

$\ell_3$  = length of inner tube between flanges

$T_T$  = temperature at top end (approx. 4°K)

$T_B$  = temperature at bottom end (approx. 80°K)

Since low temperature properties were not available for the G-10 material used for the inner and outer tubes, the thermal conductivities and coefficients of expansion of two known epoxy glass laminates<sup>3</sup> were averaged and used for preliminary analysis. Using these average properties a temperature profile was developed which satisfied boundary conditions and the incremental contractions were summed to obtain an

estimate of the total height change. The results of these calculations showed a column growth of .04 cm and a heat leak to the helium vessel of 11 milliwatts.

### Structural Analysis

Collapse Load. The inner and outer G-10 tubes are loaded in compression and should be checked for buckling. The buckling stress for a thin walled circular tube axially loaded may be calculated using the approximation<sup>4</sup>

$$S' = .3 Et/r$$

where  $S'$  = buckling stress

$E$  = modulus of elasticity

$t$  = wall thickness

$r$  = mean radius

If the buckling stress is lower than the compressive yield strength for the material being considered, the buckling stress value should be used to calculate the column collapse load.

$$P_c = A \sigma$$

where  $P_c$  = collapse load (axial)

$A$  = cross sectional area of tube

$\sigma$  = failure stress (compressive yield strength  
on buckling stress, whichever is smaller)

### Column Stiffness

By definition a column is a vertical support member normally loaded in compression. However, other loading conditions must be considered:

1. Handling and transport

2. Unbalanced magnetic forces applied to the superconducting coil
3. Shock and vibration environments

For all of the above conditions column stiffness is an important structural property which must be considered if support system capability is to be reasonably evaluated.

Axial Stiffness. The axial column deflection  $\delta$ , due to the application of axial compressive force  $P$  may be calculated using<sup>5</sup>

$$\delta = P \sum_{n=1}^3 \frac{\ell_n}{A_n E_n}$$

where  $\delta$  = axial deflection

$P$  = applied load (unit load used for calculating stiffness)

$\ell$  = tube length between flanges

$A$  = tube cross sectional area

$E$  = modulus of elasticity of material

$n$  = subscript identifying outer, intermediate and inner tubes respectively

Lateral Stiffness (bottom end fixed, top end free). The lateral influence coefficient for this condition may be determined by using the unit load method<sup>6</sup>.

$$\delta = \int \frac{m^2 d\ell}{EI} + \int \frac{kv^2 d\ell}{AG}$$

where  $\delta$  = top lateral deflection for unit lateral force applied at same location

$E$  = modulus of elasticity of material

$I$  = area moment of inertia of Section ( $\pi r^3 t$  for a thin circular section)

$d\ell$  = incremental unit of length (longitudinal)

$k$  = shape factor (2 for a thin walled circular section)

$m$  = moment distribution due to unit lateral load

$v$  = shear distribution due to unit lateral load

$G$  = modulus of rigidity

integrating the above for the 3 tube case yields

$$\delta = \frac{\ell_1}{3E_1 I_1} \left[ (\ell_1 + \ell_3 - \ell_2)^2 + (\ell_3 - \ell_2)^2 + (\ell_1 + \ell_3 - \ell_2)(\ell_3 - \ell_2) \right] + \frac{k\ell_1}{A_1 G_1} + \frac{\ell_2}{3E_2 I_2} \left[ \ell_3^2 + (\ell_2 - \ell_3)^2 - \ell_3(\ell_2 - \ell_3) \right] + \frac{k\ell_2}{A_2 G_2} + \frac{\ell_3^3}{3E_3 I_3} + \frac{k\ell_3}{A_3 G_3}$$

Lateral Stiffness (bottom end fixed, top end free to translate but no rotation). The application of column top end rotational constraints will be explained later when column systems are described. The column lateral stiffness change due to this top end rotational constraint is readily determined using the following method. A unit lateral load is applied to the column free end as before and the angular deflection of the free end due to this unit lateral load may be calculated using elementary beam theory. Then an end moment is applied to restore parallelism between the top and bottom flanges. The lateral deflection due to



this end moment is then subtracted from the "top end free" case previously solved to obtain the complete solution. The lateral stiffness of a composite column with the above rotational constraint is approximately three times greater than the free ended column.

### Tests and Results

#### Cold Test

To verify the basic concept a simple test was set-up as shown in Fig. 3.

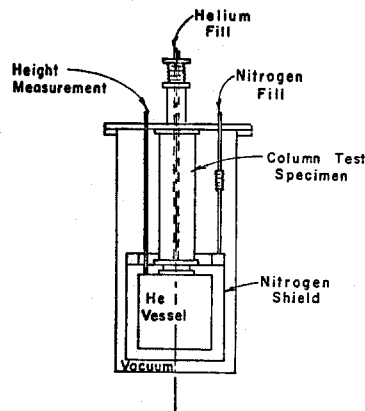


Fig. 3 Column Cold Test

The insulating vacuum chamber was pumped down and maintained below  $10^{-1}$  millitorr for all testing. A column free height measurement was taken prior to filling with liquid nitrogen and helium. After filling with cryogenics column height, temperature, and helium boil-off measurements were taken periodically for several days. Height measurements were taken with a brass rod which was inserted into the cryostat and measured while still at room temperature. Helium boil-off measurements were taken with a helium flow meter. Temperatures were measured with copper

constantan thermocouples using a liquid nitrogen cooled reference junction.

The final results showed a maximum temperature differential along the intermediate tube of  $1.5^{\circ}\text{K}$  with a total cryostat helium boil-off of .11 liquid liters per hour. Since the calculated column heat leak represented about one tenth of the total boil-off measured which seemed reasonable, no attempt was made to isolate the column boil-off from the total.

Although the column height changed appreciably during and immediately after cooldown, the final height after steady state was reached was identical to the room temperature height. This disagreement between measured and calculated height change was probably due to differences in the epoxy glass laminate properties data used for preliminary analysis and the true properties of G-10. After warm-up, the column height was again measured and no change was observed.

#### Room Temperature Tests

After completion of the cold test, the same specimen was removed from the cryostat and set-up for room temperature lateral stiffness tests as shown in Figs. 4 and 5.

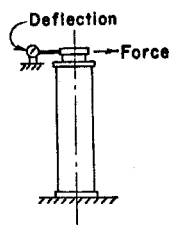


Fig. 4 Lateral Stiffness Test, Top End Free

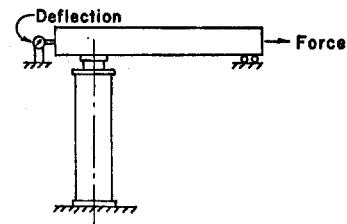


Fig. 5 Lateral Stiffness Test, Top End Free to Translate, but no rotation

The results of these tests are shown in Fig. 6.

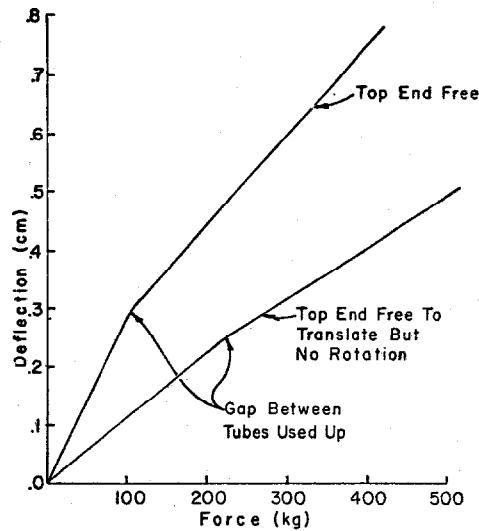


Fig. 6 Column Lateral Stiffness Test Results

Upon completion of the lateral stiffness tests the same test specimen was tested to failure by application of axial load. The results of this test are shown in Fig. 7.

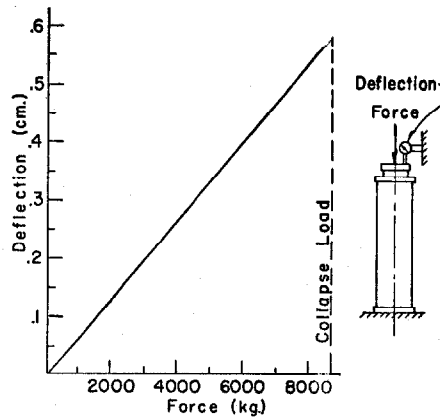


Fig. 7 Axial Stiffness and Collapse Load Test Results

#### THE GENERAL CASE

For many cryogenic support applications the basic three tube column may not be suitable in that liquid

nitrogen radiation shielding may not be used and also the space available for support structure may be limited. For such applications the low heat leak and temperature stabilization features of the previously described column may still be achieved by using many tubes of shorter length. The composite column shown in Fig. 8 using nine

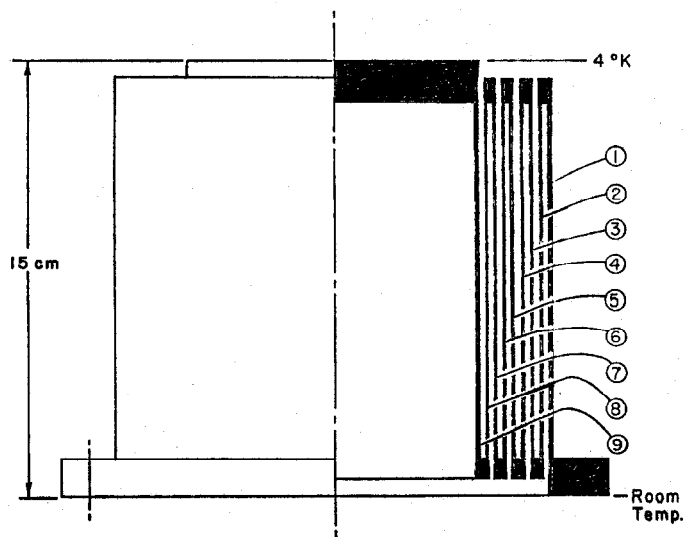


Fig. 8 Nine Tube Composite Column

concentric tubes has been chosen as a typical example for analysis. Although a wide variety of materials may be used for such column construction the following discussion is limited to two representative materials only. All metallic parts are made of 6061 aluminum in the T6 condition and all nonmetallic parts are made from epoxy glass laminates. Two types of epoxy glass laminates have been considered for which low temperature data is available. Also, to simplify analysis all tubes were assumed to have the same cross sectional area of 5 square

centimeters and radiant heat transfer between tubes has been neglected. The structural analysis approach used for the three tube case may also be used for the many tube general case. Therefore, the following discussion considers thermal analysis only.

The following approach was used for thermal analysis. An epoxy glass laminate rod of uniform cross sectional area and unknown length is sinked to room temperature at one end and 4°K at the other end. A conduction heat flow rate per unit cross sectional area is assumed to flow into the rod at the room temperature end and using thermal conductivity vs. temperature data from reference 3 the incremental rod length corresponding to unit incremental temperature decrease was calculated using Fouriers conduction equation. These data were then normalized to dimensionless length and are shown for two epoxy glass laminates in Fig. 9.

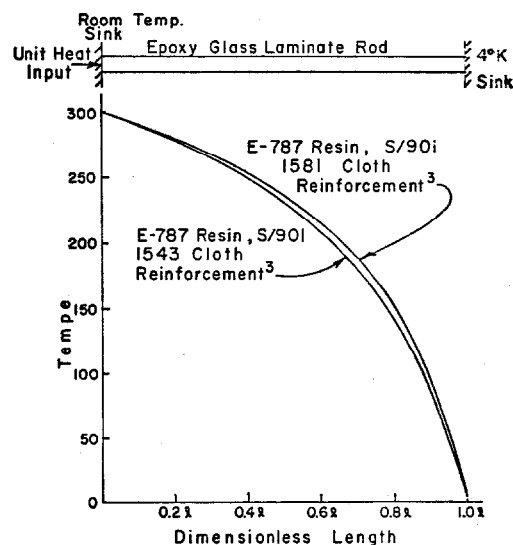


Fig. 9 Characteristic Temperature Profiles

Note that these temperature profiles are independent of cross sectional area and length (assuming uniform cross sectional area and conduction heat transfer only) whose shape is characterized by the thermal conductivity variation with temperature only. Therefore, segments of the curve may be used to represent the temperature profile between any two sinks chosen arbitrarily. Thus, if one cuts the temperature curve at 77°K, the profile to the left is representative of the temperature variation between a liquid nitrogen sink and room temperature and similarly the profile to the right is representative of the temperature variation between a liquid nitrogen sink and 4°K.

Also consider, the above rod may be cut at any location along the  $x$ -axis and a length of aluminum may be added without change to the epoxy glass laminate temperature profile. Since the thermal conductivity of aluminum is much greater than that of epoxy glass laminates the position of the temperature curve to the right of the cut will be shifted horizontally but both parts of the epoxy glass laminate temperature profile will remain unchanged in shape.

To complete the thermal analysis, length changes corresponding to the characteristic temperature profiles were calculated and the heat transferred across the 4°K boundary was determined by measuring the slope of the temperature curve at this boundary.

Table I presents the results of these calculations which shows the column heat leak and height change for seven different conditions.

Table I. Nine Tube Composite Column Analytical Results

Tube Materials	LN <sub>2</sub> Intercept Location	Epoxy Glass Laminate Material <sup>3</sup>			
		E-787 Resin S/901		E-787 Resin S/901	
	Tube Number Fig. 8	1543 Cloth Rein- forcement		1581 Cloth Rein- forcement	
		Heat Leak (Milliwatts)	Column Growth (cm)	Heat Leak (Milliwatts)	Column Growth (cm)
Even numbered tubes made of aluminum, odd numbered tubes made of epoxy glass laminates	none	60	.05	69.4	.02
	8	27.6	.06	27.8	.03
	6	13.8	.09	13.9	.05
	4	9.2	.11	9.3	.06
	2	6.9	.14	6.9	.08
All tubes epoxy glass laminates	none	34.9	-.008	38.5	-.015
Tube Number 2 aluminum all others epoxy glass laminates	2	3.9	.028	4.0	.011

Note: Negative column growth indicates shrinkage.

#### COLUMN SUPPORT SYSTEMS

For most cryogenic support applications a single column is not adequate and a system of columns would be used. Several column support systems concepts have been designed for large superconducting magnets to be used at National Accelerator Laboratory. The following discussion describes systems of two or more columns being used.

For all multiple column systems flexural hinges have been used on one or more columns to compensate for thermal contraction of the helium vessel. These flexural hinges are made of 6AL4V titanium which has a high yield strength to modulus of elasticity ratio corresponding to a high elastic strain capability. (See Appendix)

### Two Column System

A simple two column system which is presently being used on a 3 meter quadrupole magnet is shown in Fig. 10.

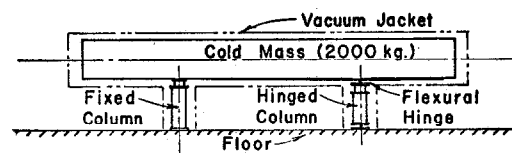


Fig. 10 Two-Column System for Three-Meter  
Quadrupole Magnet

The column on the left which is designated the "fixed column" has the top end bolted to the helium chamber and the bottom end bolted to the vacuum jacket base. The column on the right which is designated the "hinged column" is attached similarly but flexural hinges have been used both top and bottom to compensate for helium vessel shrinkage relative to the vacuum jacket. Note that the ends of the fixed column are constrained against rotation in the plane of the paper and this column would be treated analytically as "bottom end fixed, top end free to translate but no rotation" in the paper plane. However, normal to the plane of the paper both columns would be treated analytically as "bottom end fixed, top end free".



Therefore, the hinged column does not degrade support system lateral stiffness in the plane of the paper, in fact, the support system stiffness is greater in that plane.

### Three Column Systems

Two support systems concepts using three columns have been developed. The six meter long dipole magnet shown in Fig. 11 could be used as a beam transport bending

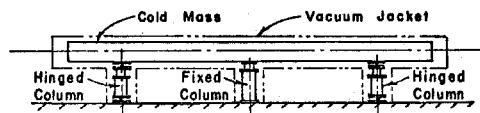


Fig. 11 Three-Column System for Six-Meter Dipole Magnet

magnet. This support system is well suited for a long slender cold mass. Note that this support system is well balanced in that the lateral stiffness in both directions are approximately equal.

Fig. 12 shows a large aperture dipole magnet which will be used as a particle spectrometer magnet. This magnet

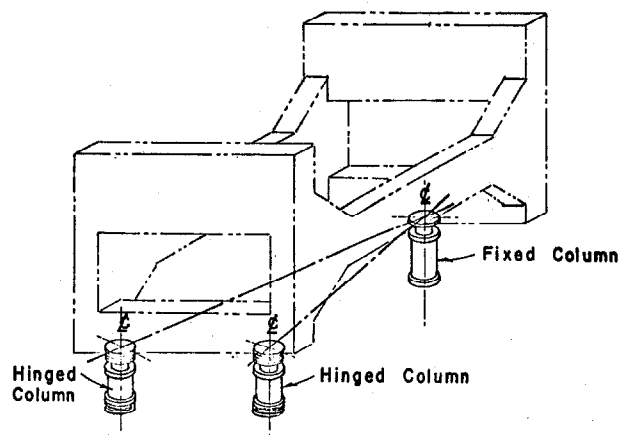


Fig. 12 Three-Column System for Spectrometer Magnet

is presently in the final construction stage and will be tested in the near future.

A fixed column has been used at the far end and two hinged columns have been used at the near side. Note that the flexural hinge axes of rotation have been aligned normal to a vertical plane which contains both a hinged column centerline and the fixed column centerline.

#### Four Column System

Fig. 13 shows a larger particle spectrometer magnet

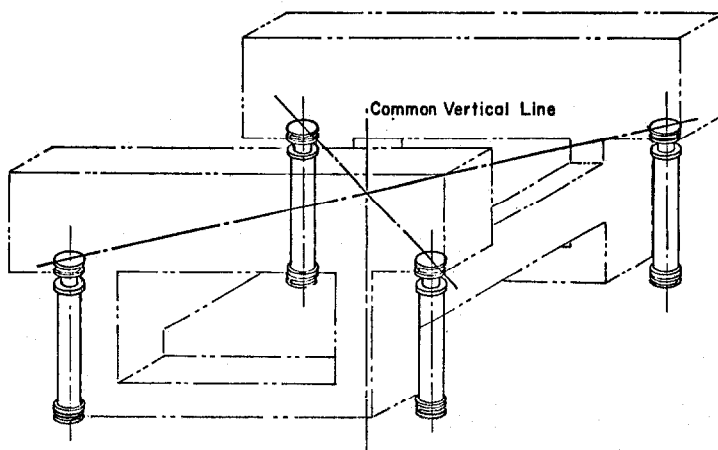


Fig. 13 Four-Column System for  
Spectrometer Magnet

which is now being designed. This support system concept uses many hinged columns and no fixed columns. Note that all flexural hinge axes of rotation have been aligned normal to vertical planes which intersect at a vertical line common to all such planes. For the four column system shown the system is balanced by locating this common vertical line equidistant from the four column centerlines.

### SUMMARY AND FUTURE PLANS

Summarizing we may say that composite columns can be used to support large cold masses with controlled thermal distortion and small heat leak through the support structure. These devices are especially well suited for large superconducting magnet applications when the magnet is floor mounted. The support structure may then be an integral part of the vacuum jacket with a composite column conveniently housed inside.

For other applications where the volume available for support structure is limited, shorter composite columns made with many tubes may be used, however, joint design should be studied and tested in more detail (e.g. the three tube column epoxy joint tested was loaded in compression only while a many tube column design may require epoxy glass laminate tension joints).

Finally, a wide variety of low conductivity materials with good mechanical properties suitable for column construction are available but low temperature data on these materials is very limited or non-existent. Therefore, a series of simple materials tests has been planned to evaluate these materials.

### ACKNOWLEDGMENTS

The author wishes to acknowledge E. H. Scholefield for his assistance in hardware design and preparation of this paper, H. L. Hart and J. J. Santori who helped with hardware fabrication and testing, and R. W. Fast for his helpful discussions and support through the course of this work.

# APPENDIX

## Flexural Hinge Design and Analysis

The hinge web geometry of the test specimen shown in Fig. 14 was sized conservatively to be used with the three tube column described previously. The specimen was made from 6AL4V titanium round stock in the annealed condition with no heat treatment after machining.

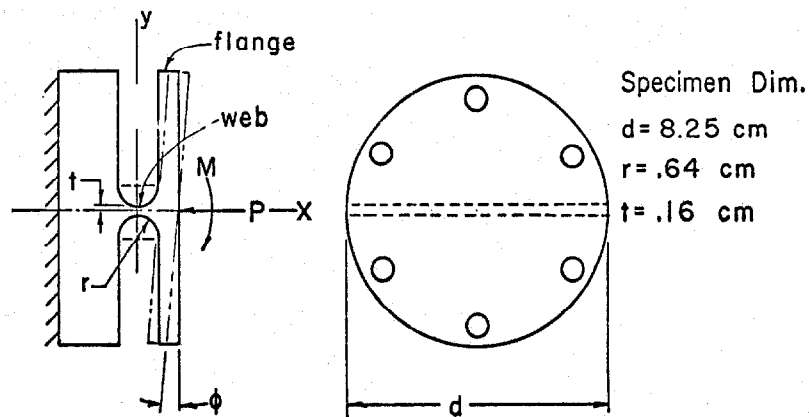


Fig. 14 Flexural Hinge Test Specimen

The following analytical approach assumes that the assumptions commonly made in the development of plate theory<sup>7</sup> hold to a reasonable degree of accuracy for the web shape shown. Following good engineering practice the maximum moment  $M$  which may be applied for elastic behavior of the hinge web is

$$M_{\max} = \frac{2}{3} \sigma_y dt^2$$

where  $\sigma_y$  = yield strength of material

$d$  = web length

$t$  = one half minimum web thickness

The following expression was then developed for the hinge rotation corresponding to  $M_{\max}$

$$\phi_{M_{\max}} = \frac{2\sigma_y (1 - \nu^2)}{E} \left(\frac{t}{r}\right)^2 f\left(\frac{t}{r}\right)$$

where  $\nu$  = poissons ratio

$E$  = modulus of elasticity

$r$  = web radius

$$f\left(\frac{t}{r}\right) = \int_0^r \frac{d\left(\frac{x}{r}\right)}{\left\{1 + \frac{t}{r} - \left[1 - \left(\frac{x}{r}\right)^2\right]^{\frac{1}{2}}\right\}^3}$$

The above integral was then evaluated numerically and a plot of  $f\left(\frac{t}{r}\right)$  as a function of  $.05 < \frac{t}{r} < 1.0$  is presented in Fig. 15.

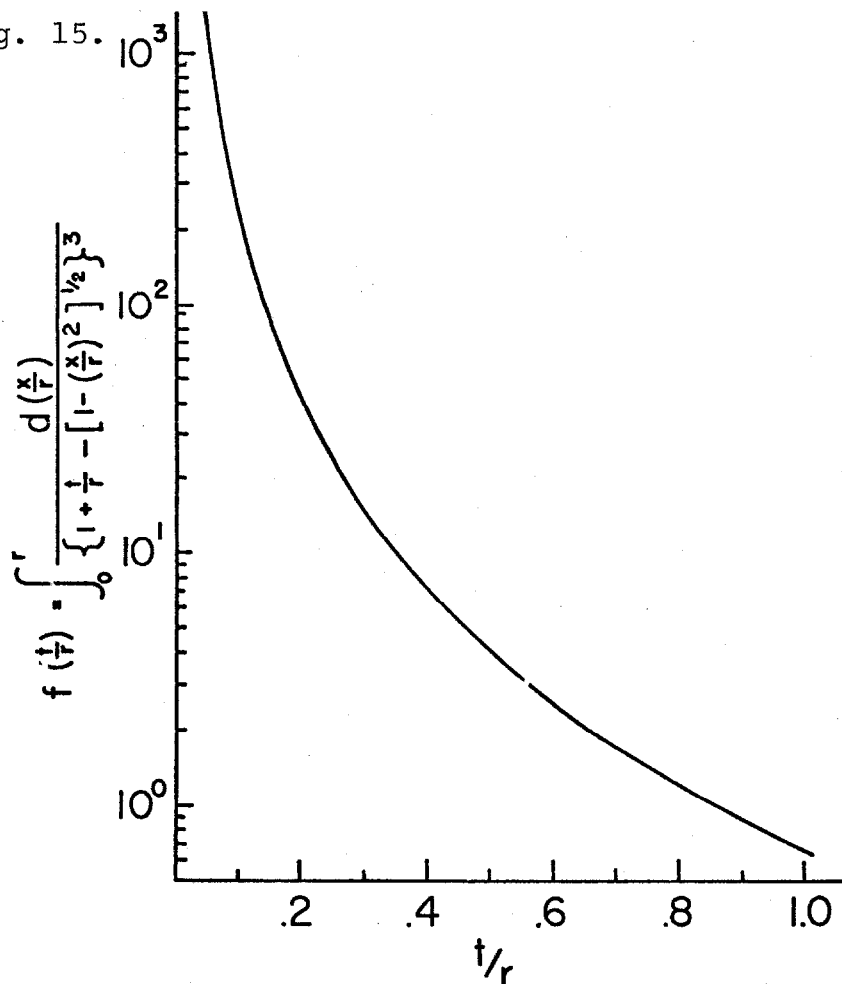


Fig. 15  $f\left(\frac{t}{r}\right)$  Integral Value

For most column support applications the flexural hinge must transmit an axial force P which reduces the hinge rotational limit for elastic behavior. The last term on the right hand side of the following equation accounts for this applied load.

$$\phi_{\max} = \frac{2\sigma_y (1 - \nu^2)}{E} \left(\frac{t}{r}\right)^2 f\left(\frac{t}{r}\right) \left(1 - \frac{P}{2dt\sigma_y}\right)$$

Where  $\phi_{\max}$  is the maximum angular deflection that the hinge will resist elastically. If the hinge is rotated through an angle greater than  $\phi_{\max}$  the hinge web will exhibit plastic deformation.

Using this equation and the web dimensions shown in Fig. 14 the test specimen rotational limit  $\phi_{\max}$  was calculated to be .023 radians for  $P = 0$ . The specimen was then tested and the web yield deflection due to the application of moment was measured to be .025 radians. Although the measured deflection was approximately 8% greater than the calculated value this agreement is considered good. One would expect the measured rotation to be greater since the hinge flange and mounting hardware are not infinitely rigid. (i.e. the hinge web was assumed to be the only flexible element in the system.)

REFERENCES

- <sup>1</sup>National Electrical Manufacturers Association Standard for Laminated Plastics. The G-10 tubing used was supplied by Richardson Company, 300 South Seventh Street, DeKalb, Illinois 60115.
- <sup>2</sup>Narmco 3170 epoxy resin with 7133 curing agent supplied by Crest Products Company, 14939 Dillow Street, Westminster, California 92683.
- <sup>3</sup>Schwartzberg, F. R., et al, Cryogenics Materials Data Handbook, AD609562, The Martin Company, Denver, Colorado, latest revision August 1968, pgs. H.1.t, H.1.V and A.13.t.
- <sup>4</sup>Roark, R. J., Formulas for Stress and Strain, Fourth Edition, pg. 352, Case 25.
- <sup>5</sup>Roark, R. J., Formulas for Stress and Strain, Fourth Edition, pg. 80, Equation 3.
- <sup>6</sup>Roark, R. J., Formulas for Stress and Strain, Fourth Edition, pg. 98, Equation 6, and pg. 129, Equation 16.
- <sup>7</sup>Timoshenko, S. and Woinowsky-Krieger, S., Theory of Plates and Shells, Second Edition, Pgs. 4, 5 and 6.